

Format for Manuscript Submission: Basic Study

Name of Journal: *World Journal of Gastroenterology*

Manuscript Type: ORIGINAL ARTICLE

Basic Study

Towards a standard diet-induced and biopsy-confirmed mouse model of non-alcoholic steatohepatitis: Impact of dietary fat source

Boland ML *et al.* Translational mouse model of non-alcoholic steatohepatitis

Michelle L Boland, Denise Oró, Kirstine S Tølbøl, Sebastian T Thrane, Jens Christian Nielsen, Taylor S Cohen, David E Tabor, Fiona Fernandes, Andrey Tovchigrechko, Sanne S Veidal, Paul Warrener, Bret R Sellman, Jacob Jelsing, Michael Feigh, Niels Vrang, James L Trevaskis, Henrik H Hansen

Michelle L Boland, Taylor S Cohen, David E Tabor, Fiona Fernandes, Andrey Tovchigrechko, Paul Warrener, Bret R Sellman, James L Trevaskis, Department of Cardiovascular, Renal and Metabolic Diseases, MedImmune, Gaithersburg, MD 20878, United States

Michelle L Boland, Denise Oró, Kirstine S Tølbøl, Sebastian T Thrane, Jens Christian Nielsen, Sanne S Veidal, Jacob Jelsing, Michael Feigh, Niels Vrang, Henrik H Hansen, Department of Pharmacology, Gubra, Hørsholm DK-2970, Denmark

Author contributions: Boland ML, Cohen TS, Warrener P, Sellman BR, Feigh M, Vrang N, Trevaskis JL, and Hansen HH designed and coordinated the study; Boland ML, Oró D, Tølbøl KS, Thrane ST, Nielsen JC, Tabor DE, and Fernandes F performed the experiments, acquired and analyzed data; Boland ML, Cohen TS, Tabor DE, Fernandes F, Oró D, Tølbøl KS, Thrane ST, Nielsen

JC, Tovchigrechko A, Veidal SS, Feigh M, Jelsing J, Vrang N, Trevaskis JL, and Hansen HH interpreted the data; Boland ML, Jelsing, Trevaskis JL, and Hansen HH wrote the manuscript; all authors approved the final version of the article.

Supported by the Innovation Fund Denmark, No. 5016-00168B (to Tølbøl KS).

Corresponding author: Henrik H Hansen, PhD, Senior Scientist, Department of Pharmacology, Gubra, Hørsholm Kongevej 11B, Hørsholm DK-2970, Denmark. hbh@gubra.dk

Abstract

BACKGROUND

The trans-fat containing amylin liver non-alcoholic steatohepatitis (NASH) (AMLN) diet has been extensively validated in C57BL/6J mice with or without the *Lep^{ob}/Lep^{ob} (ob/ob)* mutation in the leptin gene for reliably inducing metabolic and liver histopathological changes recapitulating hallmarks of NASH. Due to a recent ban on trans-fats as food additive, there is a marked need for developing a new diet capable of promoting a compatible level of disease in *ob/ob* and C57BL/6J mice.

AIM

To develop a biopsy-confirmed mouse model of NASH based on an obesogenic diet with trans-fat substituted by saturated fat.

METHODS

Male *ob/ob* mice were fed AMLN diet or a modified AMLN diet with trans-fat (Primex shortening) substituted by equivalent amounts of palm oil [Gubra amylin NASH, (GAN) diet] for 8, 12 and 16 wk. C57BL/6J mice were fed the same diets for 28 wk. AMLN and GAN diets had similar caloric content (40% fat kcal), fructose (22%) and cholesterol (2%) level.

RESULTS

The GAN diet was more obesogenic compared to the AMLN diet and impaired glucose tolerance. Biopsy-confirmed steatosis, lobular inflammation, hepatocyte ballooning, fibrotic liver lesions and hepatic transcriptome changes were similar in *ob/ob* mice fed the GAN or AMLN diet. C57BL/6J mice developed a mild to moderate fibrotic NASH phenotype when fed the same diets.

CONCLUSION

Substitution of Primex with palm oil promotes a similar phenotype of biopsy-confirmed NASH in *ob/ob* and C57BL/6J mice, making GAN diet-induced obese mouse models suitable for characterizing novel NASH treatments.

Key words: Non-alcoholic steatohepatitis; High-fat diet; Mouse model; Histopathology; Fibrosis; Liver biopsy; Liver transcriptome

Core tip: The trans-fat containing amylin liver non-alcoholic steatohepatitis (NASH) (AMLN) diet has been extensively validated in mice for reliably inducing metabolic and liver histopathological changes recapitulating hallmarks of NASH. A recent ban on trans-fats as food additive prompted the development of a new diet with similar disease-inducing properties as the AMLN diet. Here, we introduce a trans-fat-free diet high in palm oil (Gubra amylin NASH, GAN diet) that promotes a highly similar phenotype of biopsy-confirmed fibrotic NASH in both *ob/ob* and C57BL/6J mice, highlighting the suitability of GAN diet-induced obese mouse models of biopsy-confirmed NASH for the characterization of novel drug therapies for NASH.

INTRODUCTION

Liver-related complications have in recent years become widely recognized as among the most prevalent co-morbidities in obesity and diabetes. Non-alcoholic steatohepatitis (NASH) is the most severe form of non-alcoholic fatty liver disease (NAFLD), an umbrella term for a range of medical conditions with hepatic steatosis unrelated to significant alcohol consumption, use of steatogenic medication or hereditary disorders^[1]. Notably, presence of obesity, dyslipidemia and type 2 diabetes constitutes the strongest risk factors for NASH^[2,3], which has led to the concept that NASH represents the hepatic manifestation of the metabolic syndrome^[4,5]. Liver biopsies represents the gold standard method for diagnosing and grading of NASH^[6]. In NASH, lobular inflammation and liver cell damage (hepatocyte ballooning) are mandatory histopathological features in addition to steatosis^[7]. Notably, the vast majority of patients with NAFLD across the disease spectrum is asymptomatic with an unpredictable onset of NASH and with rates of fibrosis progression not linear with time. As a result, disease severity varies considerably among affected NASH patients and may progress to cirrhosis undiagnosed^[8,9]. Among the various histology - based scoring systems applied, the NAFLD activity scoring (NAS) system is the most prevalent diagnostic tool for defining NASH and assess disease activity^[10]. While not initially designed for the specific purpose of assessing therapeutic drug efficacy, the NAS system is now the most widely used scoring system in clinical trials for NASH.

The conspicuous clustering of obesity, diabetes and metabolic comorbidities in NASH patients underscores that overnutrition and dietary factors play an important role in the transition from mild NAFLD to manifest NASH. The pathogenesis of NASH is complex and multifactorial, implicating multiple parallel and converging signaling pathways. Current 'multiple-hit' hypotheses consider several insults acting sequentially or together on a background of genetical predisposition to promote NAFLD and transition to NASH. Early pathogenic events are associated with hepatic triglyceride

accumulation as result of excessive caloric intake, stimulation of hepatic *de novo* lipogenesis secondary to insulin resistance, and impaired free fatty acid clearance. Increasing triglyceride levels in hepatocytes can lead to overproduction of reactive lipid metabolites (lipotoxicity) that eventually override hepatic adaptive and regenerative mechanisms^[11-13], triggering detrimental immune cell responses with downstream activation of resident fibrogenic myofibroblasts that produce and secrete collagens^[13-15]. In the event of continuing insufficient regenerative responses, progressive extracellular matrix deposition may result in excessive fibrotic liver damage and hepatocellular cancer.

The emergence of these theories has played an important role in the development of animal models of NASH with more reproducible and robust liver histopathology. Diet-induced obese (DIO) mice fed Western diets are attractive as they recapitulate the natural history of NASH^[16]. In addition, the human NAS system largely correlates with similar histopathologic lesions in these models^[17], which makes obese mouse models of NASH increasingly employed in preclinical NASH research. Conventional obesogenic high-fat diets promote dyslipidemia, fatty liver, and mild-stage NASH without appreciable fibrosis in rodents^[16]. Hence, additional dietary stimuli ('hits') are therefore applied to enhance the pro-fibrogenic properties of the high-fat diets employed in preclinical NASH research. Among the various dietary approaches, specific modifications in Western-type obesogenic diets have consistently been reported to promote fibrotic NASH in mice. Accordingly, C57BL/6J mice fed a high-fat/fructose diet supplemented with trans-fat and cholesterol (amylin liver NASH diet, *i.e.*, AMLN diet^[18]) develop manifest NASH, characterized by steatosis, lobular inflammation and hepatocyte ballooning. Notably, a significant proportion of C57BL/6J mice fed the AMLN diet (AMLN DIO-NASH mice) develop mild to moderate fibrosis following ≥ 26 wk of feeding^[18-23]. The hepatopathology is similar, but accentuated, in leptin-deficient C57BL6J-Lep^{ob}/Lep^{ob} (*ob/ob*) mice fed the AMLN diet, demonstrating a fibrotic NASH phenotype after ≥ 12 wk of feeding^[22,24-26]. The

two AMLN DOI models of NASH have been extensively characterized in pharmacology studies with employment of biopsy-confirmed histopathology for grading and staging of baseline liver pathology^[23,24,27]. As in the clinic, DIO mouse models of NASH have unpredictable onset of disease with varying rates of progression. Consequently, any given cohort of DIO mice may represent all stages of NAFLD following long-term high-fat feeding^[18,22,28,29]. This makes it imperative to control for inherently variable dynamics in NAFLD progression that could otherwise lead to misinterpretation of data obtained in longitudinal studies. Liver biopsy procedures have therefore recently been introduced to prevent bias and enable stringent within-subject analyses in both mice^[18,22,23,27] and rats^[30].

Addition of dietary trans-fats (also called trans-unsaturated fatty acids or trans fatty acids) has been reported to enhance the steatogenic and pro-fibrotic properties of obesogenic diets in mice, including the AMLN diet^[24] and variants thereof^[21,31-33]. The underlying molecular mechanisms are not fully understood, but trans-fats may likely sensitize to the hepatotoxic effects of high-fat/carbohydrate diets by increasing insulin resistance, hepatic lipogenesis and oxidative stress^[24,32,34-36]. A recent FDA ban on trans-fats as food additive^[37], however, has prompted the development of a non-trans-fat Western diet capable of promoting metabolic and liver histopathological changes comparable to that afforded by the AMLN diet. The present study therefore aimed to develop and characterize a compatible biopsy-confirmed obese mouse model of NASH based on an isocaloric palmitic acid-enriched diet with a nutrient composition similar to the AMLN diet.

MATERIALS AND METHODS

Animals

Male *ob/ob* and C57BL/6J (C57) mice were from Jackson Laboratory (Bar Harbor, ME) or Janvier Labs (Le Genest Saint Isle, France), arrived at 5-8 wk of age and housed in a controlled environment (12 h light/dark cycle, 21 ± 2 °C, humidity 50 ± 10%). Mice were stratified and randomized to individual

diet groups according to baseline body weight and had *ad libitum* access to tap water and chow (2018 Teklad Rodent Diet, Envigo, Madison, WI; Altromin 1324, Brogaarden, Hoersholm, Denmark), AMLN diet (40 kcal-% fat (of these 22% trans-fat and 26% saturated fatty acids by weight), 22% fructose, 10% sucrose, 2% cholesterol; D09100301, Research Diets, New Brunswick, NJ, United States)^[22,24] or Gubra amylin NASH diet [GAN diet; 40 kcal-% fat (of these 0% trans-fat and 46% saturated fatty acids by weight), 22% fructose, 10% sucrose, 2% cholesterol; D09100310, Research Diets]. Mice were fed chow, AMLN or GAN diet for 8, 12 or 16 wk (*ob/ob*) and 28 wk (C57BL/6J), respectively. The study was approved by The Institutional Animal Care and Use Committee at MedImmune (Gaithersburg, MD, United States) and The Danish Animal Experiments Inspectorate (license 2013-15-2934-00784) in accordance with internationally accepted principles for the use of laboratory animals.

Body weight, body composition and liver fat mass

Body weight was monitored weekly. Whole-body fat mass was analyzed at week 8, 12 and 16 of the feeding period by non-invasive EchoMRI scanning using EchoMRI-900 (EchoMRI, Houston, TX, United States). During the scanning procedure, mice were placed in a restrainer for 90-120 s.

Intraperitoneal glucose tolerance test

An intraperitoneal glucose tolerance test (ipGTT) was performed in week 7 of the feeding period. Animals were fasted for 4 h prior to administration of the glucose bolus (1.5 g/kg). Cages were changed at the time of fasting. At $t = 0$, C57 and *ob/ob* mice received a bolus of glucose by intraperitoneal injection (5 mL/kg). Blood samples were collected from the tail vein and blood glucose was measured at time points $t = 0, 15, 30, 45, 60, 90$ and 120 min after the glucose bolus. Mice were re-fed after the last blood sampling.

Biochemical analyses

Biochemical analyses were performed as reported previously^[22,26]. Terminal plasma samples from fed animals were assayed for alanine aminotransferase (ALT), aspartate aminotransferase (AST), total triglycerides (TG) and total cholesterol. Total liver lipid mass was determined using a Bruker LF-90 minispec system (Bruker Biospin Corporation, Billerica, MA, United States) and expressed relative (%) to total liver weight.

Liver biopsy

A separate cohort of *ob/ob* mice were fed AMLN or GAN diet for 9 wk before a liver biopsy procedure was applied as described in detail previously^[22]. On the surgery day, mice were anesthetized with isoflurane (2%-3%, in 100% oxygen), a small abdominal incision in the midline was made, and the left lateral lobe of the liver was exposed. A cone-shaped wedge of liver tissue (50-100 mg) was excised from the distal part of the lobe. The cut surface of the liver was closed by electrosurgical bipolar coagulation using an electrosurgical unit (ERBE VIO 100C, ERBE, Marietta, GA, United States). The liver was returned to the abdominal cavity, the abdominal wall was sutured and skin stapled. Carprofen (5 mg/kg, i.p.) was administered at the time of surgery and at post-operative day one and two. After the procedure, animals were single-housed and kept on the respective diet for a total period of 16 wk.

Liver histology and digital image analysis

Biopsy and terminal liver samples (both from the left lateral lobe) were fixed overnight in 4% paraformaldehyde. Liver tissue was paraffin-embedded and sectioned (3 μ m thickness). Sections were stained with hematoxylin-eosin (HE, Dako, Glostrup, Denmark), Picro-Sirius red (Sigma-Aldrich, Broendby, Denmark), anti-galectin-3 (cat. 125402, Biolegend, San Diego, CA, United States), or anti-type I collagen (Col1a1; cat. 1310-01, Southern Biotech, Birmingham, AL, United States) using standard procedures^[22,23]. The NAS and fibrosis staging system was applied to liver pre-biopsies and terminal samples for scoring of steatosis, lobular inflammation, hepatocyte ballooning,

and fibrosis outlined by Kleiner *et al*^[10]. Quantitative histomorphometry was analyzed using digital imaging software (VIS Software, Visiopharm, Hørsholm, Denmark)^[22,23]. Proportional (fractional) areas of liver fat (HE-staining), galectin-3 and Col1a1 were expressed relative to total sectional area. All histological assessments were performed by histologists blinded to the experimental groups.

RNA sequencing

Liver transcriptome analysis was performed by RNA sequencing on RNA extracts from terminal liver samples (15 mg fresh tissue), as described in detail elsewhere^[22,23]. The RNA quantity was measured using Qubit[®] (Thermo Scientific, Eugene, OR, United States). The RNA quality was determined using a bioanalyzer with RNA 6000 Nano kit (Agilent, Waldbronn, Germany). RNA sequence libraries were prepared with NeoPrep (Illumina, San Diego, CA, United States) using Illumina TruSeq stranded mRNA Library kit for NeoPrep (Illumina, San Diego, CA, United States) and sequenced on the NextSeq 500 (Illumina, San Diego, CA, United States) with NSQ 500 hi-Output KT v2 (75 CYS, Illumina, San Diego, CA, United States). Reads were aligned to the GRCm38 v84 Ensembl Mus musculus genome using STAR v.2.5.2a with default parameters^[38]. Differential gene expression analysis was performed with DEseq2³⁷. Genes with a Benjamini and Hochberg adjusted $P \leq 0.05$ (5% false discovery rate, FDR) were regarded as statistically significantly regulated. The Reactome pathway database^[39] was used as gene annotation in a gene set analysis using the R package PIANO v.1.18.1^[40], with the Stouffer method and Benjamini-Hochberg adjusted P values (FDR < 0.01).

Statistical analyses

Except for RNA sequencing, data were analyzed using GraphPad Prism v7.03 software (GraphPad, La Jolla, CA, United States). All results are shown as mean \pm standard error of mean. A two-way ANOVA with Tukey's multiple comparisons test was performed for body weight and quantitative

histological analyses. A one-way ANOVA with Dunnett's post-hoc test was used for all other parameters. A P value < 0.05 was considered statistically significant.

RESULTS

Metabolic changes in ob/ob mice fed GAN or AMLN diet for up to 16 wk

The temporal progression of metabolic deficits was determined in *ob/ob* mice fed the GAN (GAN *ob/ob*-NASH) or AMLN (AMLN *ob/ob*-NASH) diet for up to 16 wk. Body weight curves were significantly different in GAN and AMLN *ob/ob*-NASH mice (overall $P < 0.001$, two-way ANOVA). Compared to the AMLN diet, the GAN diet induced greater body weight gain in *ob/ob* mice from diet week 7 and onwards (Figure 1A). Relative body weight gain over the 16-week feeding period was $141.6 \pm 2.9\%$ (GAN *ob/ob*-NASH) and $125.2 \pm 3.6\%$ (AMLN *ob/ob*-NASH). GAN-*ob/ob* mice displayed more pronounced increases in whole-body fat mass at all time points measured (Figure 1B). The GAN and AMLN diets promoted similar degree of hepatomegaly in *ob/ob* mice (Figure 1C). An ipGTT was performed in diet week 7 and demonstrated impaired glucose tolerance in GAN, but not AMLN, *ob/ob*-NASH mice compared to chow-fed C57 controls (Figure 1D and E). During the ipGTT, plasma insulin levels were equally elevated in GAN and AMLN *ob/ob*-NASH mice (Figure 1F). Plasma ALT and AST levels were significantly increased in GAN and AMLN *ob/ob*-NASH mice after 8 wk on the diet and did not change further during the 16-wk feeding period. The GAN and AMLN diets promoted a similar degree of hypercholesterolemia (diet week 8-16, $P < 0.05$) in *ob/ob* mice with slightly reduced TG levels (diet week 16, $P < 0.05$), as compared to chow-fed C57 mice (Table 1).

Terminal liver lipid levels in GAN and AMLN *ob/ob*-NASH mice were approximately 10-fold higher than that of age-matched C57 mice and were maximally elevated after 8 weeks of feeding (Table 1). In addition to metabolic changes, the gut microbiome composition in GAN and AMLN *ob/ob* mice was characterized by bacterial 16S rRNA gene sequencing performed on

serial fecal samples. The GAN and AMLN diets promoted similar taxonomic shifts compared to baseline (chow feeding). The structural modulation of the gut microbiota was largely manifest two weeks after the change to GAN or AMLN diet, being slightly more accentuated following 16 wk of feeding (Supplemental Figure 1). Compared to baseline, the changes in microbiome composition in GAN and AMLN *ob/ob* mice was mainly driven by increases in the relative abundance of *Akkermansia*, *Bacteroides* and *Parasutterella* with reciprocal decreases in *Clostridiales* and *Porphyromonadaceae*. Consistently lowered relative abundance of *Lactobacillus* was also observed in GAN *ob/ob*-NASH mice.

Biopsy-confirmed progression of liver histopathology in ob/ob mice fed GAN or AMLN diet for 16 wk

Liver histopathological changes in GAN *ob/ob* mice were assessed in *ob/ob* mice fed GAN or AMLN diet for 16 wk ($n = 8-10$ per group). A liver biopsy was sampled after 9 wk on the respective diet for within-subject analysis of disease progression. Representative histological stainings are shown in Figure 2A. Comparable changes in composite NAS and fibrosis scores from feeding week 9 to 16 were observed in GAN *ob/ob* and AMLN *ob/ob* mice (Figure 2B). At feeding week 9, GAN *ob/ob* and AMLN *ob/ob* mice showed mild-to-moderate fibrosis (F1-F2) with an equal distribution of mice progressing in fibrosis severity. A major proportion of GAN or AMLN diet fed *ob/ob* mice demonstrated moderate fibrosis after 16 weeks of feeding (Figure 2C). Individual pre-biopsy and terminal histopathological scores on steatosis, lobular inflammation and hepatocyte ballooning are indicated in Supplemental Figure 2. Steatosis severity was severe (score 3) and sustained after 9 weeks of feeding in both GAN and AMLN *ob/ob*-NASH mice. Both diets induced moderate-grade (score 2) lobular inflammation in almost all *ob/ob* mice without significant changes from feeding week 9 to 16. The rate of hepatocyte ballooning was low in *ob/ob* mice fed the GAN or AMLN diet for 9 weeks, however, increased during the remainder of the feeding period.

Hepatocyte ballooning did not progress beyond grade 1 in *ob/ob* mice. Terminal quantitative histopathological changes were also similar in *ob/ob* mice fed the GAN or AMLN diet, as indicated by morphometric analyses of steatosis, inflammation and Col1a1 (Figure 3).

Liver transcriptome changes in ob/ob mice fed AMLN or GAN diet for 16 wk

To characterize the effect of 16-week feeding on global liver gene expression, the transcriptome of GAN and AMLN *ob/ob*-NASH mice vs. chow-fed C57 mice were analyzed by RNA sequencing. To assess the overall similarity of the individual transcriptome samples, a principal component analysis (PCA) was performed. The primary PCA (accounting for the major variability in the data set) yielded conspicuous clustering of transcriptome samples from GAN and AMLN *ob/ob*-NASH mice, being clearly separated from chow-fed C57 controls (Figure 4A), indicating that the two NASH-promoting diets overall promoted substantial, however highly similar, alterations in liver global gene signatures of *ob/ob* mice. In accordance, a total pool of 9725 and 9760 differentially expressed genes (DEGs) were identified in GAN and AMLN *ob/ob*-NASH mice, respectively, with virtually all regulated genes being shared in the two *ob/ob*-NASH groups (Figure 4B). For initial evaluation of the DEGs identified, we probed for candidate gene transcripts associated with NASH and fibrosis (see Supplemental Table 1). GAN and AMLN *ob/ob*-NASH mice showed significant and overlapping regulations of candidate genes (Figure 4C), particularly associated to modulated fatty acid synthesis (*Fasn*, *Scd1*), reduced fatty acid β -oxidation (*Cpt-1*), lowered triglyceride synthesis (*Gpat4*), reduced cholesterol synthesis (*Hmgcr*, *Hmgcs1*) and transport (*ApoCIII*, *Ldlr*, *Lrp1*, *Scarb1*); impaired insulin (*Akt*, *Irs1*, *Irs2*) and FXR (*Cyp7a1*, *Cyp8b1*, *Ostb*) signaling; enhanced monocyte differentiation/recruitment (*Ccr1*, *Ccr2*, *Cd14*, *Cd68*, *Cd86*, *Il1a*, *Il1a*, *Mac-2*, *Mcp-1*), pro-inflammatory signaling (*Nfkb*, *P38*, *Tgfbr*, *Tnfa*); inflammasome (*Ipaf*, *Nlrp1b*, *Nlrp3*, *Tlr4*) and pro-apoptotic activity (*Casp-8*, *Rip-1*, *Rip-3*), and enhanced extracellular matrix (ECM) reorganization (*a-Sma*, *Col1a1*, *Col1a2*, *Col3a1*, *Col5a1/2/3*, *Col6a1/2/3*, *Mmp2*,

Mmp13, *Timp1/2/3*). When performing a group-wise comparison of global gene expression profiles in GAN vs. AMLN *ob/ob* mice, liver transcriptome signatures were distinguished by only nine DEGs (*Ces3b*, *Cfhr1*, *Cyp1a1*, *Cyp2f2*, *Gm4788*, *Keg1*, *Serpina3k*, *Ugt1a9*, *Ugt2a3*). To obtain further resolution of the liver transcriptome changes in GAN and AMLN *ob/ob*-NASH mice vs. chow-fed C57 controls, a gene set enrichment analysis was subsequently conducted. The Reactome gene annotation analysis identified several disease-relevant biological pathways significantly enriched in both GAN and AMLN *ob/ob*-NASH mice. Notably, all significantly enriched pathways were completely overlapping between GAN and AMLN *ob/ob*-NASH mice (Figure 4D).

Liver histopathology in C57 mice fed GAN or AMLN diet for 28 wk

To investigate liver histological changes in wild-type mice, C57 mice were fed chow ($n = 15$), GAN ($n = 30$) or AMLN ($n = 30$) diet for 28 wk. Histopathological scores and proportionate area of *Col1a1* are shown in Figure 5. GAN and AMLN diets were both highly obesogenic in C57 (GAN DIO-NASH, AMLN DIO-NASH) mice. GAN DIO-NASH mice showed significantly higher endpoint body weight (46.0 ± 0.8 g) compared to AMLN DIO-NASH (40.6 ± 0.6 g, $P < 0.001$) and chow-fed C57 mice (30.7 ± 0.4 g, $P < 0.001$ vs GAN DIO-NASH and AMLN-DIO NASH mice). While age-matched chow-fed C57 mice displayed normal liver histology, GAN DIO-NASH mice developed severe steatosis (score 3, 30/30 mice) and moderate-to-severe lobular inflammation (score 0, 1/30 mice; score 1, 3/30 mice; score 2, 19/30 mice; score 3, 7/30 mice) upon 28 wk of feeding (Figure 5A and B). Hepatocyte ballooning was largely absent in GAN DIO-NASH mice (score 0, 26/30 mice; score 1, 4/30 mice, Figure 5C). Generally, a NAS of 5-6 was observed in GAN DIO-NASH mice (score 3, 1/30 mice; score 4, 3/30 mice; score 5, 17/30 mice; score 6, 7/30 mice; score 7, 2/30 mice, Figure 5D). Fibrosis was typically mild to moderate in GAN DIO-NASH mice (F0, 1/30 mice; F1, 10/30 mice; F2, 18/30 mice; F3, 1/30 mice), see Figure 5E. AMLN

DIO-NASH mice showed a liver histological phenotype very similar to GAN DIO-NASH mice, as indicated by severe steatosis (score 3, 30/30 mice), moderate to severe lobular inflammation (score 0, 1/30 mice; score 1, 3/30 mice; score 2, 19/30 mice; score 3, 7/30 mice), inconsistent hepatocyte ballooning (score 0, 17/30 mice; score 1, 13/30 mice), and mild-to-moderate fibrosis (F0, 3/30 mice; F1, 4/30 mice; F2, 23/30 mice; F3, 0/30 mice). In addition, *Col1a1* proportionate areas were increased to a similar degree in GAN and AMLN DIO-NASH mice, as compared to chow-fed C57 mice, see Figure 5F.

DISCUSSION

The AMLN DIO-NASH and *ob/ob*-NASH mouse models have been extensively validated and characterized in an increasing number of pharmacology studies. Here, we compared the metabolic and liver histological phenotype in *ob/ob* mice fed the AMLN diet or a modified AMLN diet (GAN diet) with Primex shortening, a trans-fat containing food additive, substituted with equivalent amounts of palm oil. The GAN and AMLN diets promoted similar biopsy-confirmed liver lesions with hallmarks of fibrotic NASH in both *ob/ob* and C57 mice. Hence, the maintained NASH phenotype in both *ob/ob* and C57 mice indicates the utility of GAN DIO mouse models of biopsy-confirmed NASH for the preclinical characterization of novel drug therapies for NASH.

The composition of the AMLN diet, containing high levels of saturated fat, fructose, trans-fat and cholesterol, reflects dietary factors considered important in the pathogenesis of NAFLD/NASH. Accordingly, excess energy intake from dietary fat and simple sugars (Western diets) has been strongly linked to NAFLD/NASH^[41,42]. In particular, increased consumption of saturated fats and fructose has been associated with the deleterious effects of intrahepatic lipid accumulation, enhanced lipogenesis, insulin resistance, hepatocyte oxidative stress and inflammation in NAFLD/NASH^[43-47]. Although less well-characterized in NASH, *trans*-unsaturated fat

consumption and dietary cholesterol may sensitize to the hepatotoxic effects of excessive fat and fructose intake^[31,32,48,49]. Because the FDA has recently imposed a ban on the use of trans-fat additives in foods, this prompted us to develop a compatible mouse model of NASH based on an obesogenic diet high in saturated fat and with a nutrient composition and caloric density similar to the AMLN diet.

The GAN and AMLN diets were both highly obesogenic in *ob/ob* mice. Notably, weight gain and adiposity were even more pronounced in mice fed the GAN diet. Other high-fat/trans-fat diets have been reported inducing slightly less weight gain in wild-type mice compared to trans-fat-free hypercaloric diets^[36]. Although not specifically addressed in the present study, it may be speculated that substitution of trans-fat with palm oil led to improved diet palatability and/or fat absorption rates. This is also indirectly supported by the observation that hyperphagic *ob/ob* mice fed the AMLN diet attain slightly less weight gain compared to chow feeding^[22,23]. Consistent with previous reports^[22,24,27], the AMLN diet did not influence glucose homeostasis in *ob/ob* mice which contrasts findings of mild glucose intolerance in obese wild-type mice fed other high-fat/trans-fat diet types^[31,36,50]. The AMLN diet has been reported to elevate endogenous glucose production in C57 mice^[51], suggesting development of peripheral insulin resistance. As also C57 mice fed the AMLN diet maintain normal oral glucose tolerance^[22,24], it may be speculated that glucoregulatory effects of trans-fats depend on the composition of trans-fat species in obesogenic diets. In contrast, GAN *ob/ob*-NASH mice displayed significantly impaired glucose tolerance compared to chow-fed C57 mice, indicating a more robust insulin-resistant phenotype in GAN *ob/ob*-NASH mice. Because insulin resistance is closely associated with NAFLD and is recognized as an important pathophysiological factor in the progression to NASH^[52-54], this lends further support to the translatability of the GAN *ob/ob*-NASH mouse model. It should be noted that GAN and AMLN *ob/ob*-NASH mice both showed suppressed expression of hepatic genes related to lipid and glucose handling. This points to the possibility that

extrahepatic mechanisms contribute to impaired glucose handling in GAN *ob/ob*-NASH mice. GAN and AMLN *ob/ob*-NASH mice demonstrated similarly profound hyperinsulinemia, which argues for sustained pancreatic β -cell compensation in both models. Importantly, however, glucose intolerance in leptin-deficient *ob/ob* mice has been attributed to failure to suppress hepatic glucose production in conjunction with impaired muscle glucose uptake, likely precipitated by defective triglyceride handling in these tissues^[55-57]. In addition, *ob/ob* mice show impaired glucose uptake in adipose tissues^[58,59]. Although the present study did not specifically determine insulin sensitivity by hyperinsulinemic-euglycemic clamp techniques, the marked adipogenic properties of the GAN diet may therefore promote insulin resistance at both the hepatic and extrahepatic level to facilitate manifest glucose intolerance in GAN *ob/ob*-NASH mice.

Consistent with the obese phenotype in GAN and AMLN *ob/ob*-NASH mice, the two models demonstrated pronounced hepatomegaly and intrahepatic lipid accumulation. Development of hypercholesterolemia, but not hypertriglyceridemia, was also a shared feature in GAN and AMLN *ob/ob*-NASH mice, possibly attributed to suppressed hepatic triglyceride secretion, as high dietary cholesterol intake can downregulate hepatic cholesterol ester and lipoprotein synthesis^[60,61]. This is supported by our finding of reduced expression of several hepatic genes involved in cholesterol synthesis and transport. Enhanced hepatic fat uptake combined with impaired capacity to secrete fatty acids may thus be important mechanisms leading to marked steatosis in GAN and AMLN *ob/ob* mice. Hepatic injury was suggested by increased levels of plasma transaminases in GAN and AMLN *ob/ob* mice, subsequently confirmed by liver histology. We have previously reported that *ob/ob* mice develop reliably manifest NASH when maintained on AMLN diet for a relatively short feeding period (≥ 12 wk). The AMLN *ob/ob*-NASH model is characterized by biopsy-confirmed severe hepatic steatosis, moderate to severe lobular inflammation, mild hepatocyte ballooning and fibrotic lesions increasing in severity with prolonged feeding periods^[22,24-26], recapitulating

clinical histopathological criteria for the diagnosis of fibrosing NASH^[7,62]. Also, the AMLN *ob/ob*-NASH model has been extensively characterized in pharmacology studies^[23-25,27]. Notably, *ob/ob* mice fed the GAN and AMLN diet, respectively, developed a highly similar fibrotic NASH phenotype with comparable within-subject disease progression rates during the feeding period. Accordingly, GAN and AMLN-*ob/ob*-NASH mice demonstrated similar liver histopathology, as determined by both standard clinical histopathological scoring and imaging-based quantitative histological assessment of steatosis, inflammation and fibrosis.

The GAN and AMLN diets induced virtually identical hepatic transcriptome signatures with marked alterations in candidate genes associated with NAFLD/NASH. An unsupervised analysis for full-scale mapping and functional annotation of liver transcriptome signatures confirmed completely overlapping GAN and AMLN diet-induced hepatic signaling pathway perturbations with signatures of inefficient intrahepatic lipid and carbohydrate handling, stimulated immune cell activity, increased apoptotic activity, ECM remodeling and cell cycle modulation. In addition to suppressed transcription of genes associated with cholesterol metabolism (discussed above), a subset of genes involved in fatty acid catabolism (β -oxidation) and storage (triglyceride synthesis) were also downregulated. This could indirectly suggest free fatty acid overload and defective lipid compartmentation, which has been associated with hepatocyte cytotoxicity (lipotoxicity), inflammation and apoptosis in NASH^[11-13]. Also, increased immune activity and hepatocyte damage was supported by upregulation of genes involved in monocyte differentiation/recruitment, pro-inflammatory cytokine production, inflammasome activation and pro-apoptotic signaling. The significant upregulation of α -Sma, multiple collagen isoforms (Col1a1, Col1a2, Col3a1, Col5a1/2/3, Col6a1/2/3) and molecules involved in ECM reorganization (Mmp2, Mmp13, Timp1/2/3), suggests that hepatic collagen accumulation in GAN and AMLN *ob/ob*-NASH mice is a combined effect of stimulated fibrogenesis and altered balance between the activity of collagen-

degrading matrix metalloproteinases and tissue inhibitors of metalloproteinases.

The observation that the GAN and AMLN diets both promoted consistent fibrotic NASH in *ob/ob* mice indicates that palm oil supplementation fully compensated for the lack of trans-fat in the GAN diet. The extent of hepatic saturated fatty acid accumulation parallels disease severity in NAFLD/NASH patients^[63], and inefficient disposal of saturated free fatty acids is considered hepatotoxic^[64,65]. Specifically, the particularly high levels of palmitic acid in the GAN diet (37% of total fat by weight) compared to the AMLN diet (17% of total fat by weight) invites the possibility that this nutritional component played an integral role in the development and progression of liver pathology in GAN *ob/ob*-NASH mice. In support of this view, high palmitic acid (palmitate at physiological pH) levels in hepatocytes and non-parenchymal liver cells can trigger substantial lipotoxic damage through various mechanism associated with NASH pathology, including oxidative stress^[66], endoplasmic reticulum stress^[67], pro-apoptotic signaling^[68] as well as Kupffer cell^[69] and hepatic stellate cell activation^[70]. In addition to direct cytotoxicity, hepatic palmitic acid overload can also promote hepatotoxic effects via increased formation palmitate-derived complex lipids, including ceramides^[71]. Interestingly, long-term AMLN diet feeding has been reported to elevate hepatic levels of palmitate-containing ceramides in C57 mice, most likely due to incomplete mitochondrial fatty acid oxidation nutritional as result of nutritional overload^[20].

Compared to AMLN *ob/ob*-NASH mice, longer AMLN diet feeding periods (≥ 26 wk) are required for inducing consistent fibrotic NASH in C57 mice^[18,19,22,23], which is likely explained by hyperphagia-driven excessive AMLN diet intake in leptin-deficient *ob/ob*-NASH mice. A comparative study was therefore also performed in C57 mice fed the GAN or AMLN diet for 28 wk (DIO-NASH mice). Similar to *ob/ob* mice, C57 mice showed significantly greater weight gain when fed the GAN diet compared to AMLN diet. Histological assessments of biopsied liver specimens revealed highly

compatible liver lesions in GAN and AMLN DIO-NASH mice. Both models presented with manifest NASH (NAS \geq 4), characterized by severe steatosis, moderate-to-severe lobular inflammation. In GAN DIO-NASH mice, fibrosis stage was mild to moderate with significantly increased proportionate area of *Colla1* compared to chow-fed C57 mice showing normal liver histology. Consistent with previously reported studies in AMLN DIO-NASH mice^[23,72], hepatocyte ballooning was only detected in a subset of GAN and AMLN DIO-NASH mice. In addition to the GAN diet, other isocaloric variants of the AMLN diet were tested for the ability to induce a metabolic and NASH phenotype comparable to the AMLN diet. Compared to the GAN diet, *ob/ob* and C57 mice did not consistently develop fibrotic NASH when fed these diets, including diets supplemented with trans-fat from partially hydrogenated corn oil (Supplemental Table 2). As the trans-fatty acids (largely *trans*-oleic acid) in the AMLN diet are derived from partially hydrogenated soybean and palm oils, the differences in liver histopathology may therefore relate to the source of dietary fat used to prepare the partially hydrogenated vegetable oil.

We also characterized the gut microbiome composition in *ob/ob* mice fed the GAN and AMLN diet. GAN and AMLN *ob/ob*-NASH mice exhibited a similar gut microbiome signature, which further emphasizes the comparable phenotype in GAN and AMLN *ob/ob*-NASH mice. Both high-fat diets promoted sustained bacterial taxonomic shifts which were evident only two weeks after switching from chow feeding. Other high-fat diet feeding regimens have been reported to induce rapid gut microbiome structural changes in mice^[73-75], suggesting that dietary fat played a major role in modulating gut bacterial communities in GAN and AMLN *ob/ob*-NASH mice. At the genus level, the microbiome signature in GAN and AMLN *ob/ob*-NASH mice was dominated by increased abundance of *Bacteroides* and *Akkermansia* paralleled by reductions in unclassified *Porphyromonadaceae*. Although various fecal microbiome profiles have been associated with NASH^[76], recent studies have indicated increased *Bacteroides*^[77-79] and reduced *Porphyromonadaceae*^[80]

abundance in NASH patients compared to healthy control subjects. *Bacteroides* have a large number and diversity of genes encoding enzymes converting complex polysaccharides to short-chain fatty acids that serve as energy substrates and signaling molecules^[81,82]. Increased energy harvest from bacterial degradation of dietary polysaccharides has been suggested to contribute to adiposity in *ob/ob* mice^[83]. In addition, *Bacteroides* and *Akkermansia* include prominent mucosa-degrading species^[84], which have been linked to modulation of gut barrier integrity and immune responses in obesity-associated diseases, including NASH^[85,86]. It should be considered that high-fat diet feeding has been reported to promote similar gut microbiome signatures in obesity-prone and obesity-resistant mice, which signifies efficient gut ecosystem adaptations to dietary changes independent of the metabolic phenotype^[87]. Given the early and stable changes in dominant gut bacterial genera following the shift from chow to GAN/AMLN diet feeding, it cannot be ruled out that microbial adaptive responses secondary to altered nutrient intake played a role in shaping the gut microbiome in GAN and AMLN *ob/ob* mice.

CONCLUSION

In conclusion, modification of the AMLN diet by substitution of Primex shortening with palm oil (GAN diet) resulted in a maintained NASH phenotype in both *ob/ob* and C57 mice. The GAN diet was more obesogenic than the AMLN diet in both *ob/ob* and C57 mice and impaired glucose intolerance in *ob/ob* mice. Hence, the clear metabolic and histopathological hallmarks of NASH in *ob/ob* and C57 mice fed the GAN diet highlights the suitability of these mouse model for characterizing novel drug therapies for NASH.

ACKNOWLEDGEMENTS

The authors would like to acknowledge Benji Gill, Stephanie Oldham (MedImmune, Gaithersburg, MD), Mikkel Christensen-Dalsgaard and Lillian Petersen (Gubra) for skillful technical assistance.

REFERENCES

- 1 **Bedossa P.** Current histological classification of NAFLD: Strength and limitations. *Hepatol Int* 2013; **7 Suppl 2**: 765-770 [PMID: 26202292 DOI: 10.1007/s12072-013-9446-z]
- 2 **Angulo P,** Keach JC, Batts KP, Lindor KD. Independent predictors of liver fibrosis in patients with nonalcoholic steatohepatitis. *Hepatology* 1999; **30**: 1356-1362 [PMID: 10573511 DOI: 10.1002/hep.510300604]
- 3 **Ratziu V,** Giral P, Charlotte F, Bruckert E, Thibault V, Theodorou I, Khalil L, Turpin G, Opolon P, Poynard T. Liver fibrosis in overweight patients. *Gastroenterology* 2000; **118**: 1117-1123 [PMID: 10833486 DOI: 10.1016/S0016-5085(00)70364-7]
- 4 **Younossi ZM,** Koenig AB, Abdelatif D, Fazel Y, Henry L, Wymer M. Global epidemiology of nonalcoholic fatty liver disease-Meta-analytic assessment of prevalence, incidence, and outcomes. *Hepatology* 2016; **64**: 73-84 [PMID: 26707365 DOI: 10.1002/hep.28431]
- 5 **Tilg H,** Moschen AR, Roden M. NAFLD and diabetes mellitus. *Nat Rev Gastroenterol Hepatol* 2017; **14**: 32-42 [PMID: 27729660 DOI: 10.1038/nrgastro.2016.147]
- 6 **Bedossa P.** Diagnosis of non-alcoholic fatty liver disease/non-alcoholic steatohepatitis: Why liver biopsy is essential. *Liver Int* 2018; **38 Suppl 1**: 64-66 [PMID: 29427497 DOI: 10.1111/liv.13653]
- 7 **Bedossa P.** Pathology of non-alcoholic fatty liver disease. *Liver Int* 2017; **37 Suppl 1**: 85-89 [PMID: 28052629 DOI: 10.1111/liv.13301]
- 8 **McPherson S,** Hardy T, Henderson E, Burt AD, Day CP, Anstee QM. Evidence of NAFLD progression from steatosis to fibrosing-steatohepatitis using paired biopsies: Implications for prognosis and clinical management. *J Hepatol* 2015; **62**: 1148-1155 [PMID: 25477264 DOI: 10.1016/j.jhep.2014.11.034]

- 9 **Singh S**, Allen AM, Wang Z, Prokop LJ, Murad MH, Loomba R. Fibrosis progression in nonalcoholic fatty liver vs nonalcoholic steatohepatitis: A systematic review and meta-analysis of paired-biopsy studies. *Clin Gastroenterol Hepatol* 2015; **13**: 643-54.e1-9; quiz e39-40 [PMID: 24768810 DOI: 10.1016/j.cgh.2014.04.014]
- 10 **Kleiner DE**, Brunt EM, Van Natta M, Behling C, Contos MJ, Cummings OW, Ferrell LD, Liu YC, Torbenson MS, Unalp-Arida A, Yeh M, McCullough AJ, Sanyal AJ; Nonalcoholic Steatohepatitis Clinical Research Network. Design and validation of a histological scoring system for nonalcoholic fatty liver disease. *Hepatology* 2005; **41**: 1313-1321 [PMID: 15915461 DOI: 10.1002/hep.20701]
- 11 **Rosso N**, Chavez-Tapia NC, Tiribelli C, Bellentani S. Translational approaches: From fatty liver to non-alcoholic steatohepatitis. *World J Gastroenterol* 2014; **20**: 9038-9049 [PMID: 25083077 DOI: 10.3748/wjg.v20.i27.9038]
- 12 **Berlanga A**, Guiu-Jurado E, Porrás JA, Auguet T. Molecular pathways in non-alcoholic fatty liver disease. *Clin Exp Gastroenterol* 2014; **7**: 221-239 [PMID: 25045276 DOI: 10.2147/CEG.S62831]
- 13 **Friedman SL**, Neuschwander-Tetri BA, Rinella M, Sanyal AJ. Mechanisms of NAFLD development and therapeutic strategies. *Nat Med* 2018; **24**: 908-922 [PMID: 29967350 DOI: 10.1038/s41591-018-0104-9]
- 14 **Tsuchida T**, Friedman SL. Mechanisms of hepatic stellate cell activation. *Nat Rev Gastroenterol Hepatol* 2017; **14**: 397-411 [PMID: 28487545 DOI: 10.1038/nrgastro.2017.38]
- 15 **Szabo G**, Petrasek J. Inflammasome activation and function in liver disease. *Nat Rev Gastroenterol Hepatol* 2015; **12**: 387-400 [PMID: 26055245 DOI: 10.1038/nrgastro.2015.94]
- 16 **Hansen HH**, Feigh M, Veidal SS, Rigbolt KT, Vrang N, Fosgerau K. Mouse models of nonalcoholic steatohepatitis in preclinical drug development. *Drug Discov Today* 2017; **22**: 1707-1718 [PMID: 28687459 DOI: 10.1016/j.drudis.2017.06.007]

- 17 **Liang W**, Menke AL, Driessen A, Koek GH, Lindeman JH, Stoop R, Havekes LM, Kleemann R, van den Hoek AM. Establishment of a general NAFLD scoring system for rodent models and comparison to human liver pathology. *PLoS One* 2014; **9**: e115922 [PMID: 25535951 DOI: 10.1371/journal.pone.0115922]
- 18 **Clapper JR**, Hendricks MD, Gu G, Wittmer C, Dolman CS, Herich J, Athanacio J, Villescaz C, Ghosh SS, Heilig JS, Lowe C, Roth JD. Diet-induced mouse model of fatty liver disease and nonalcoholic steatohepatitis reflecting clinical disease progression and methods of assessment. *Am J Physiol Gastrointest Liver Physiol* 2013; **305**: G483-G495 [PMID: 23886860 DOI: 10.1152/ajpgi.00079.2013]
- 19 **Ding ZM**, Xiao Y, Wu X, Zou H, Yang S, Shen Y, Xu J, Workman HC, Usborne AL, Hua H. Progression and Regression of Hepatic Lesions in a Mouse Model of NASH Induced by Dietary Intervention and Its Implications in Pharmacotherapy. *Front Pharmacol* 2018; **9**: 410 [PMID: 29765319 DOI: 10.3389/fphar.2018.00410]
- 20 **Patterson RE**, Kalavalapalli S, Williams CM, Nautiyal M, Mathew JT, Martinez J, Reinhard MK, McDougall DJ, Rocca JR, Yost RA, Cusi K, Garrett TJ, Sunny NE. Lipotoxicity in steatohepatitis occurs despite an increase in tricarboxylic acid cycle activity. *Am J Physiol Endocrinol Metab* 2016; **310**: E484-E494 [PMID: 26814015 DOI: 10.1152/ajpendo.00492.2015]
- 21 **Kawashita E**, Ishihara K, Nomoto M, Taniguchi M, Akiba S. A comparative analysis of hepatic pathological phenotypes in C57BL/6J and C57BL/6N mouse strains in non-alcoholic steatohepatitis models. *Sci Rep* 2019; **9**: 204 [PMID: 30659241 DOI: 10.1038/s41598-018-36862-7]
- 22 **Kristiansen MN**, Veidal SS, Rigbolt KT, Tølbøl KS, Roth JD, Jelsing J, Vrang N, Feigh M. Obese diet-induced mouse models of nonalcoholic steatohepatitis-tracking disease by liver biopsy. *World J Hepatol* 2016; **8**: 673-684 [PMID: 27326314 DOI: 10.4254/wjh.v8.i16.673]
- 23 **Tølbøl KS**, Kristiansen MN, Hansen HH, Veidal SS, Rigbolt KT, Gillum MP, Jelsing J, Vrang N, Feigh M. Metabolic and hepatic effects of liraglutide,

obeticholic acid and elafibranor in diet-induced obese mouse models of biopsy-confirmed nonalcoholic steatohepatitis. *World J Gastroenterol* 2018; **24**: 179-194 [PMID: 29375204 DOI: 10.3748/wjg.v24.i2.179]

24 **Trevaskis JL**, Griffin PS, Wittmer C, Neuschwander-Tetri BA, Brunt EM, Dolman CS, Erickson MR, Napora J, Parkes DG, Roth JD. Glucagon-like peptide-1 receptor agonism improves metabolic, biochemical, and histopathological indices of nonalcoholic steatohepatitis in mice. *Am J Physiol Gastrointest Liver Physiol* 2012; **302**: G762-G772 [PMID: 22268099 DOI: 10.1152/ajpgi.00476.2011]

25 **Jouihan H**, Will S, Guionaud S, Boland ML, Oldham S, Ravn P, Celeste A, Trevaskis JL. Superior reductions in hepatic steatosis and fibrosis with co-administration of a glucagon-like peptide-1 receptor agonist and obeticholic acid in mice. *Mol Metab* 2017; **6**: 1360-1370 [PMID: 29107284 DOI: 10.1016/j.molmet.2017.09.001]

26 **Boland ML**, Oldham S, Boland BB, Will S, Lapointe JM, Guionaud S, Rhodes CJ, Trevaskis JL. Nonalcoholic steatohepatitis severity is defined by a failure in compensatory antioxidant capacity in the setting of mitochondrial dysfunction. *World J Gastroenterol* 2018; **24**: 1748-1765 [PMID: 29713129 DOI: 10.3748/wjg.v24.i16.1748]

27 **Roth JD**, Feigh M, Veidal SS, Fensholdt LK, Rigbolt KT, Hansen HH, Chen LC, Petitjean M, Friley W, Vrang N, Jelsing J, Young M. INT-767 improves histopathological features in a diet-induced ob/ob mouse model of biopsy-confirmed non-alcoholic steatohepatitis. *World J Gastroenterol* 2018; **24**: 195-210 [PMID: 29375205 DOI: 10.3748/wjg.v24.i2.195]

28 **Farrell GC**, Mridha AR, Yeh MM, Arsov T, Van Rooyen DM, Brooling J, Nguyen T, Heydet D, Delghingaro-Augusto V, Nolan CJ, Shackel NA, McLennan SV, Teoh NC, Larter CZ. Strain dependence of diet-induced NASH and liver fibrosis in obese mice is linked to diabetes and inflammatory phenotype. *Liver Int* 2014; **34**: 1084-1093 [PMID: 24107103 DOI: 10.1111/liv.12335]

29 **Haczeyni F**, Poekes L, Wang H, Mridha AR, Barn V, Geoffrey Haigh W,

Ioannou GN, Yeh MM, Leclercq IA, Teoh NC, Farrell GC. Obeticholic acid improves adipose morphometry and inflammation and reduces steatosis in dietary but not metabolic obesity in mice. *Obesity (Silver Spring)* 2017; **25**: 155-165 [PMID: 27804232 DOI: 10.1002/oby.21701]

30 **Tølbøl KS**, Stierstorfer B, Rippmann JF, Veidal SS, Rigbolt KTG, Schönberger T, Gillum MP, Hansen HH, Vrang N, Jelsing J, Feigh M, Broermann A. Disease Progression and Pharmacological Intervention in a Nutrient-Deficient Rat Model of Nonalcoholic Steatohepatitis. *Dig Dis Sci* 2019; **64**: 1238-1256 [PMID: 30511198 DOI: 10.1007/s10620-018-5395-7]

31 **Tetri LH**, Basaranoglu M, Brunt EM, Yerian LM, Neuschwander-Tetri BA. Severe NAFLD with hepatic necroinflammatory changes in mice fed trans fats and a high-fructose corn syrup equivalent. *Am J Physiol Gastrointest Liver Physiol* 2008; **295**: G987-G995 [PMID: 18772365 DOI: 10.1152/ajpgi.90272.2008]

32 **Machado RM**, Stefano JT, Oliveira CP, Mello ES, Ferreira FD, Nunes VS, de Lima VM, Quintão EC, Catanozi S, Nakandakare ER, Lottenberg AM. Intake of trans fatty acids causes nonalcoholic steatohepatitis and reduces adipose tissue fat content. *J Nutr* 2010; **140**: 1127-1132 [PMID: 20357081 DOI: 10.3945/jn.109.117937]

33 **Obara N**, Fukushima K, Ueno Y, Wakui Y, Kimura O, Tamai K, Kakazu E, Inoue J, Kondo Y, Ogawa N, Sato K, Tsuduki T, Ishida K, Shimosegawa T. Possible involvement and the mechanisms of excess trans-fatty acid consumption in severe NAFLD in mice. *J Hepatol* 2010; **53**: 326-334 [PMID: 20462650 DOI: 10.1016/j.jhep.2010.02.029]

34 **Morinaga M**, Kon K, Saito H, Arai K, Kusama H, Uchiyama A, Yamashina S, Ikejima K, Watanabe S. Sodium 4-phenylbutyrate prevents murine dietary steatohepatitis caused by trans-fatty acid plus fructose. *J Clin Biochem Nutr* 2015; **57**: 183-191 [PMID: 26566303 DOI: 10.3164/jcbn.15-75]

35 **Ibrahim A**, Natrajan S, Ghafoorunissa R. Dietary trans-fatty acids alter adipocyte plasma membrane fatty acid composition and insulin sensitivity in rats. *Metabolism* 2005; **54**: 240-246 [PMID: 15789505 DOI: 10.1016/j.metabol.2004.08.019]

- 36 **Koppe SW**, Elias M, Moseley RH, Green RM. Trans fat feeding results in higher serum alanine aminotransferase and increased insulin resistance compared with a standard murine high-fat diet. *Am J Physiol Gastrointest Liver Physiol* 2009; **297**: G378-G384 [PMID: 19541924 DOI: 10.1152/ajpgi.90543.2008]
- 37 **US Food Drug Administration**. Final Determination Regarding Partially Hydrogenated Oils (Removing Trans Fat). 2018. Available from: <https://www.federalregister.gov/documents/2018/05/21/2018-10714/final-determination-regarding-partially-hydrogenated-oils>
- 38 **Dobin A**, Davis CA, Schlesinger F, Drenkow J, Zaleski C, Jha S, Batut P, Chaisson M, Gingeras TR. STAR: Ultrafast universal RNA-seq aligner. *Bioinformatics* 2013; **29**: 15-21 [PMID: 23104886 DOI: 10.1093/bioinformatics/bts635]
- 39 **Fabregat A**, Jupe S, Matthews L, Sidiropoulos K, Gillespie M, Garapati P, Haw R, Jassal B, Korninger F, May B, Milacic M, Roca CD, Rothfels K, Sevilla C, Shamovsky V, Shorser S, Varusai T, Viteri G, Weiser J, Wu G, Stein L, Hermjakob H, D'Eustachio P. The Reactome Pathway Knowledgebase. *Nucleic Acids Res* 2018; **46**: D649-D655 [PMID: 29145629 DOI: 10.1093/nar/gkx1132]
- 40 **Väremo L**, Nielsen J, Nookaew I. Enriching the gene set analysis of genome-wide data by incorporating directionality of gene expression and combining statistical hypotheses and methods. *Nucleic Acids Res* 2013; **41**: 4378-4391 [PMID: 23444143 DOI: 10.1093/nar/gkt111]
- 41 **Oddy WH**, Herbison CE, Jacoby P, Ambrosini GL, O'Sullivan TA, Ayonrinde OT, Olynyk JK, Black LJ, Beilin LJ, Mori TA, Hands BP, Adams LA. The Western dietary pattern is prospectively associated with nonalcoholic fatty liver disease in adolescence. *Am J Gastroenterol* 2013; **108**: 778-785 [PMID: 23545714 DOI: 10.1038/ajg.2013.95]
- 42 **Asrih M**, Jornayvaz FR. Diets and nonalcoholic fatty liver disease: The good and the bad. *Clin Nutr* 2014; **33**: 186-190 [PMID: 24262589 DOI: 10.1016/j.clnu.2013.11.003]
- 43 **Lim JS**, Mietus-Snyder M, Valente A, Schwarz JM, Lustig RH. The role of fructose in the pathogenesis of NAFLD and the metabolic syndrome. *Nat Rev*

Gastroenterol Hepatol 2010; 7: 251-264 [PMID: 20368739 DOI: 10.1038/nrgastro.2010.41]

44 **Alkhoury N**, Dixon LJ, Feldstein AE. Lipotoxicity in nonalcoholic fatty liver disease: Not all lipids are created equal. *Expert Rev Gastroenterol Hepatol* 2009; 3: 445-451 [PMID: 19673631 DOI: 10.1586/egh.09.32]

45 **Abdelmalek MF**, Suzuki A, Guy C, Unalp-Arida A, Colvin R, Johnson RJ, Diehl AM; Nonalcoholic Steatohepatitis Clinical Research Network. Increased fructose consumption is associated with fibrosis severity in patients with nonalcoholic fatty liver disease. *Hepatology* 2010; 51: 1961-1971 [PMID: 20301112 DOI: 10.1002/hep.23535]

46 **Moore JB**, Gunn PJ, Fielding BA. The role of dietary sugars and de novo lipogenesis in non-alcoholic fatty liver disease. *Nutrients* 2014; 6: 5679-5703 [PMID: 25514388 DOI: 10.3390/nu6125679]

47 **Della Pepa G**, Vetrani C, Lombardi G, Bozzetto L, Annuzzi G, Rivellese AA. Isocaloric Dietary Changes and Non-Alcoholic Fatty Liver Disease in High Cardiometabolic Risk Individuals. *Nutrients* 2017; 9 pii: E1065 [PMID: 28954437 DOI: 10.3390/nu9101065]

48 **Walenberg SM**, Shiri-Sverdlov R. Cholesterol is a significant risk factor for non-alcoholic steatohepatitis. *Expert Rev Gastroenterol Hepatol* 2015; 9: 1343-1346 [PMID: 26395315 DOI: 10.1586/17474124.2015.1092382]

49 **Jeyapal S**, Putcha UK, Mullapudi VS, Ghosh S, Sakamuri A, Kona SR, Vadakattu SS, Madakasira C, Ibrahim A. Chronic consumption of fructose in combination with trans fatty acids but not with saturated fatty acids induces nonalcoholic steatohepatitis with fibrosis in rats. *Eur J Nutr* 2018; 57: 2171-2187 [PMID: 28676973 DOI: 10.1007/s00394-017-1492-1]

50 **Zhao X**, Shen C, Zhu H, Wang C, Liu X, Sun X, Han S, Wang P, Dong Z, Ma X, Hu K, Sun A, Ge J. Trans-Fatty Acids Aggravate Obesity, Insulin Resistance and Hepatic Steatosis in C57BL/6 Mice, Possibly by Suppressing the IRS1 Dependent Pathway. *Molecules* 2016; 21: pii: E705 [PMID: 27248994 DOI: 10.3390/molecules21060705]

51 **Kalavalapalli S**, Bril F, Guingab J, Vergara A, Garrett TJ, Sunny NE, Cusi K.

Impact of exenatide on mitochondrial lipid metabolism in mice with nonalcoholic steatohepatitis. *J Endocrinol* 2019; **241**: 293-305 [PMID: 31082799 DOI: 10.1530/JOE-19-0007]

52 **Marchesini G**, Brizi M, Morselli-Labate AM, Bianchi G, Bugianesi E, McCullough AJ, Forlani G, Melchionda N. Association of nonalcoholic fatty liver disease with insulin resistance. *Am J Med* 1999; **107**: 450-455 [PMID: 10569299 DOI: 10.1016/S0002-9343(99)00271-5]

53 **Loomba R**, Abraham M, Unalp A, Wilson L, Lavine J, Doo E, Bass NM; Nonalcoholic Steatohepatitis Clinical Research Network. Association between diabetes, family history of diabetes, and risk of nonalcoholic steatohepatitis and fibrosis. *Hepatology* 2012; **56**: 943-951 [PMID: 22505194 DOI: 10.1002/hep.25772]

54 **Williams CD**, Stengel J, Asike MI, Torres DM, Shaw J, Contreras M, Landt CL, Harrison SA. Prevalence of nonalcoholic fatty liver disease and nonalcoholic steatohepatitis among a largely middle-aged population utilizing ultrasound and liver biopsy: A prospective study. *Gastroenterology* 2011; **140**: 124-131 [PMID: 20858492 DOI: 10.1053/j.gastro.2010.09.038]

55 **Haluzik M**, Colombo C, Gavrilova O, Chua S, Wolf N, Chen M, Stannard B, Dietz KR, Le Roith D, Reitman ML. Genetic background (C57BL/6J versus FVB/N) strongly influences the severity of diabetes and insulin resistance in ob/ob mice. *Endocrinology* 2004; **145**: 3258-3264 [PMID: 15059949 DOI: 10.1210/en.2004-0219]

56 **Grefhorst A**, van Dijk TH, Hammer A, van der Sluijs FH, Havinga R, Havekes LM, Romijn JA, Groot PH, Reijngoud DJ, Kuipers F. Differential effects of pharmacological liver X receptor activation on hepatic and peripheral insulin sensitivity in lean and ob/ob mice. *Am J Physiol Endocrinol Metab* 2005; **289**: E829-E838 [PMID: 15941783 DOI: 10.1152/ajpendo.00165.2005]

57 **Muurling M**, Mensink RP, Pijl H, Romijn JA, Havekes LM, Voshol PJ. Rosiglitazone improves muscle insulin sensitivity, irrespective of increased triglyceride content, in ob/ob mice. *Metabolism* 2003; **52**: 1078-1083 [PMID:

12898477 DOI: 10.1016/s0026-0495(03)00109-4]

58 **Tan SX**, Fisher-Wellman KH, Fazakerley DJ, Ng Y, Pant H, Li J, Meoli CC, Coster AC, Stöckli J, James DE. Selective insulin resistance in adipocytes. *J Biol Chem* 2015; **290**: 11337-11348 [PMID: 25720492 DOI: 10.1074/jbc.M114.623686]

59 **Jager J**, Corcelle V, Grémeaux T, Laurent K, Waget A, Pagès G, Binétruy B, Le Marchand-Brustel Y, Burcelin R, Bost F, Tanti JF. Deficiency in the extracellular signal-regulated kinase 1 (ERK1) protects leptin-deficient mice from insulin resistance without affecting obesity. *Diabetologia* 2011; **54**: 180-189 [PMID: 20953578 DOI: 10.1007/s00125-010-1944-0]

60 **Henkel J**, Coleman CD, Schraplau A, Jöhrens K, Weber D, Castro JP, Hugo M, Schulz TJ, Krämer S, Schürmann A, Püschel GP. Induction of steatohepatitis (NASH) with insulin resistance in wildtype B6 mice by a western-type diet containing soybean oil and cholesterol. *Mol Med* 2017; **23**: 70-82 [PMID: 28332698 DOI: 10.2119/molmed.2016.00203]

61 **Ma K**, Malhotra P, Soni V, Hedroug O, Annaba F, Dudeja A, Shen L, Turner JR, Khramtsova EA, Saksena S, Dudeja PK, Gill RK, Alrefai WA. Overactivation of intestinal SREBP2 in mice increases serum cholesterol. *PLoS One* 2014; **9**: e84221 [PMID: 24465397 DOI: 10.1371/journal.pone.0084221]

62 **Brown GT**, Kleiner DE. Histopathology of nonalcoholic fatty liver disease and nonalcoholic steatohepatitis. *Metabolism* 2016; **65**: 1080-1086 [PMID: 26775559 DOI: 10.1016/j.metabol.2015.11.008]

63 **Chiappini F**, Coilly A, Kadar H, Gual P, Tran A, Desterke C, Samuel D, Duclos-Vallée JC, Touboul D, Bertrand-Michel J, Brunelle A, Guettier C, Le Naour F. Metabolism dysregulation induces a specific lipid signature of nonalcoholic steatohepatitis in patients. *Sci Rep* 2017; **7**: 46658 [PMID: 28436449 DOI: 10.1038/srep46658]

64 **Mota M**, Banini BA, Cazanave SC, Sanyal AJ. Molecular mechanisms of lipotoxicity and glucotoxicity in nonalcoholic fatty liver disease. *Metabolism* 2016; **65**: 1049-1061 [PMID: 26997538 DOI: 10.1016/j.metabol.2016.02.014]

65 **Liangpunsakul S**, Chalasani N. Lipid mediators of liver injury in nonalcoholic fatty liver disease. *Am J Physiol Gastrointest Liver Physiol* 2019; **316**:

G75-G81 [PMID: 30383414 DOI: 10.1152/ajpgi.00170.2018]

66 **Zhang K**, Kim H, Fu Z, Qiu Y, Yang Z, Wang J, Zhang D, Tong X, Yin L, Li J, Wu J, Qi NR, Houten SM, Zhang R. Deficiency of the Mitochondrial NAD Kinase Causes Stress-Induced Hepatic Steatosis in Mice. *Gastroenterology* 2018; **154**: 224-237 [PMID: 28923496 DOI: 10.1053/j.gastro.2017.09.010]

67 **Wei Y**, Wang D, Topczewski F, Pagliassotti MJ. Saturated fatty acids induce endoplasmic reticulum stress and apoptosis independently of ceramide in liver cells. *Am J Physiol Endocrinol Metab* 2006; **291**: E275-E281 [PMID: 16492686 DOI: 10.1152/ajpendo.00644.2005]

68 **Cazanave SC**, Mott JL, Bronk SF, Werneburg NW, Fingas CD, Meng XW, Finnberg N, El-Deiry WS, Kaufmann SH, Gores GJ. Death receptor 5 signaling promotes hepatocyte lipoapoptosis. *J Biol Chem* 2011; **286**: 39336-39348 [PMID: 21941003 DOI: 10.1074/jbc.M111.280420]

69 **Luo W**, Xu Q, Wang Q, Wu H, Hua J. Effect of modulation of PPAR- γ activity on Kupffer cells M1/M2 polarization in the development of non-alcoholic fatty liver disease. *Sci Rep* 2017; **7**: 44612 [PMID: 28300213 DOI: 10.1038/srep44612]

70 **Hetherington AM**, Sawyez CG, Zilberman E, Stoianov AM, Robson DL, Borradaile NM. Differential Lipotoxic Effects of Palmitate and Oleate in Activated Human Hepatic Stellate Cells and Epithelial Hepatoma Cells. *Cell Physiol Biochem* 2016; **39**: 1648-1662 [PMID: 27626926 DOI: 10.1159/000447866]

71 **Hirsova P**, Ibrahim SH, Gores GJ, Malhi H. Lipotoxic lethal and sublethal stress signaling in hepatocytes: Relevance to NASH pathogenesis. *J Lipid Res* 2016; **57**: 1758-1770 [PMID: 27049024 DOI: 10.1194/jlr.R066357]

72 **Honda Y**, Imajo K, Kato T, Kessoku T, Ogawa Y, Tomeno W, Kato S, Mawatari H, Fujita K, Yoneda M, Saito S, Nakajima A. The Selective SGLT2 Inhibitor Ipragliflozin Has a Therapeutic Effect on Nonalcoholic Steatohepatitis in Mice. *PLoS One* 2016; **11**: e0146337 [PMID: 26731267 DOI: 10.1371/journal.pone.0146337]

73 **Turnbaugh PJ**, Ridaura VK, Faith JJ, Rey FE, Knight R, Gordon JI. The effect of diet on the human gut microbiome: A metagenomic analysis in

humanized gnotobiotic mice. *Sci Transl Med* 2009; **1**: 6ra14 [PMID: 20368178 DOI: 10.1126/scitranslmed.3000322]

74 **Zheng X**, Huang F, Zhao A, Lei S, Zhang Y, Xie G, Chen T, Qu C, Rajani C, Dong B, Li D, Jia W. Bile acid is a significant host factor shaping the gut microbiome of diet-induced obese mice. *BMC Biol* 2017; **15**: 120 [PMID: 29241453 DOI: 10.1186/s12915-017-0462-7]

75 **Frank DN**, Bales ES, Monks J, Jackman MJ, MacLean PS, Ir D, Robertson CE, Orlicky DJ, McManaman JL. Perilipin-2 Modulates Lipid Absorption and Microbiome Responses in the Mouse Intestine. *PLoS One* 2015; **10**: e0131944 [PMID: 26147095 DOI: 10.1371/journal.pone.0131944]

76 **de Faria Ghatti F**, Oliveira DG, de Oliveira JM, de Castro Ferreira LEVV, Cesar DE, Moreira APB. Influence of gut microbiota on the development and progression of nonalcoholic steatohepatitis. *Eur J Nutr* 2018; **57**: 861-876 [PMID: 28875318 DOI: 10.1007/s00394-017-1524-x]

77 **Wong VW**, Tse CH, Lam TT, Wong GL, Chim AM, Chu WC, Yeung DK, Law PT, Kwan HS, Yu J, Sung JJ, Chan HL. Molecular characterization of the fecal microbiota in patients with nonalcoholic steatohepatitis--a longitudinal study. *PLoS One* 2013; **8**: e62885 [PMID: 23638162 DOI: 10.1371/journal.pone.0062885]

78 **Zhu L**, Baker SS, Gill C, Liu W, Alkhouri R, Baker RD, Gill SR. Characterization of gut microbiomes in nonalcoholic steatohepatitis (NASH) patients: A connection between endogenous alcohol and NASH. *Hepatology* 2013; **57**: 601-609 [PMID: 23055155 DOI: 10.1002/hep.26093]

79 **Boursier J**, Mueller O, Barret M, Machado M, Fizanne L, Araujo-Perez F, Guy CD, Seed PC, Rawls JF, David LA, Hunault G, Oberti F, Calès P, Diehl AM. The severity of nonalcoholic fatty liver disease is associated with gut dysbiosis and shift in the metabolic function of the gut microbiota. *Hepatology* 2016; **63**: 764-775 [PMID: 26600078 DOI: 10.1002/hep.28356]

80 **Da Silva HE**, Teterina A, Comelli EM, Taibi A, Arendt BM, Fischer SE, Lou W, Allard JP. Nonalcoholic fatty liver disease is associated with dysbiosis independent of body mass index and insulin resistance. *Sci Rep* 2018; **8**: 1466

[PMID: 29362454 DOI: 10.1038/s41598-018-19753-9]

81 **El Kaoutari A**, Armougom F, Gordon JI, Raoult D, Henrissat B. The abundance and variety of carbohydrate-active enzymes in the human gut microbiota. *Nat Rev Microbiol* 2013; **11**: 497-504 [PMID: 23748339 DOI: 10.1038/nrmicro3050]

82 **Koh A**, De Vadder F, Kovatcheva-Datchary P, Bäckhed F. From Dietary Fiber to Host Physiology: Short-Chain Fatty Acids as Key Bacterial Metabolites. *Cell* 2016; **165**: 1332-1345 [PMID: 27259147 DOI: 10.1016/j.cell.2016.05.041]

83 **Turnbaugh PJ**, Ley RE, Mahowald MA, Magrini V, Mardis ER, Gordon JI. An obesity-associated gut microbiome with increased capacity for energy harvest. *Nature* 2006; **444**: 1027-1031 [PMID: 17183312 DOI: 10.1038/nature05414]

84 **Donaldson GP**, Lee SM, Mazmanian SK. Gut biogeography of the bacterial microbiota. *Nat Rev Microbiol* 2016; **14**: 20-32 [PMID: 26499895 DOI: 10.1038/nrmicro3552]

85 **Miura K**, Ohnishi H. Role of gut microbiota and Toll-like receptors in nonalcoholic fatty liver disease. *World J Gastroenterol* 2014; **20**: 7381-7391 [PMID: 24966608 DOI: 10.3748/wjg.v20.i23.7381]

86 **Derrien M**, Belzer C, de Vos WM. Akkermansia muciniphila and its role in regulating host functions. *Microb Pathog* 2017; **106**: 171-181 [PMID: 26875998 DOI: 10.1016/j.micpath.2016.02.005]

87 **Hildebrandt MA**, Hoffmann C, Sherrill-Mix SA, Keilbaugh SA, Hamady M, Chen YY, Knight R, Ahima RS, Bushman F, Wu GD. High-fat diet determines the composition of the murine gut microbiome independently of obesity. *Gastroenterology* 2009; **137**: 1716-24.e1-2 [PMID: 19706296 DOI: 10.1053/j.gastro.2009.08.042]

Footnotes

Institutional review board statement: The study was reviewed and approved by the Institutional Review Board at MedImmune and Gubra.

Institutional animal care and use committee statement: All animal experiments conformed to the internationally accepted principles for the care and use of laboratory animals (licence No. 2013-15-2934-00784, The Animal Experiments Inspectorate, Denmark; protocol no. MI-17-0005, The Institutional Animal Care and Use Committee at MedImmune, Gaithersburg, MD, United States).

Conflict-of-interest statement: Michelle L. Boland and James L. Trevaskis were previously employed by MedImmune, LLC. Taylor S. Cohen, David Tabor, Fiona Fernandes, Andrey Tovchigrechko, Paul Warrener, and Bret R. Sellman are employed by MedImmune LLC. All other authors have nothing to disclose.

Data sharing statement: No additional data are available.

ARRIVE guidelines statement: The authors have read the ARRIVE guidelines, and the manuscript was prepared and revised according to the ARRIVE guidelines.

Figure Legends

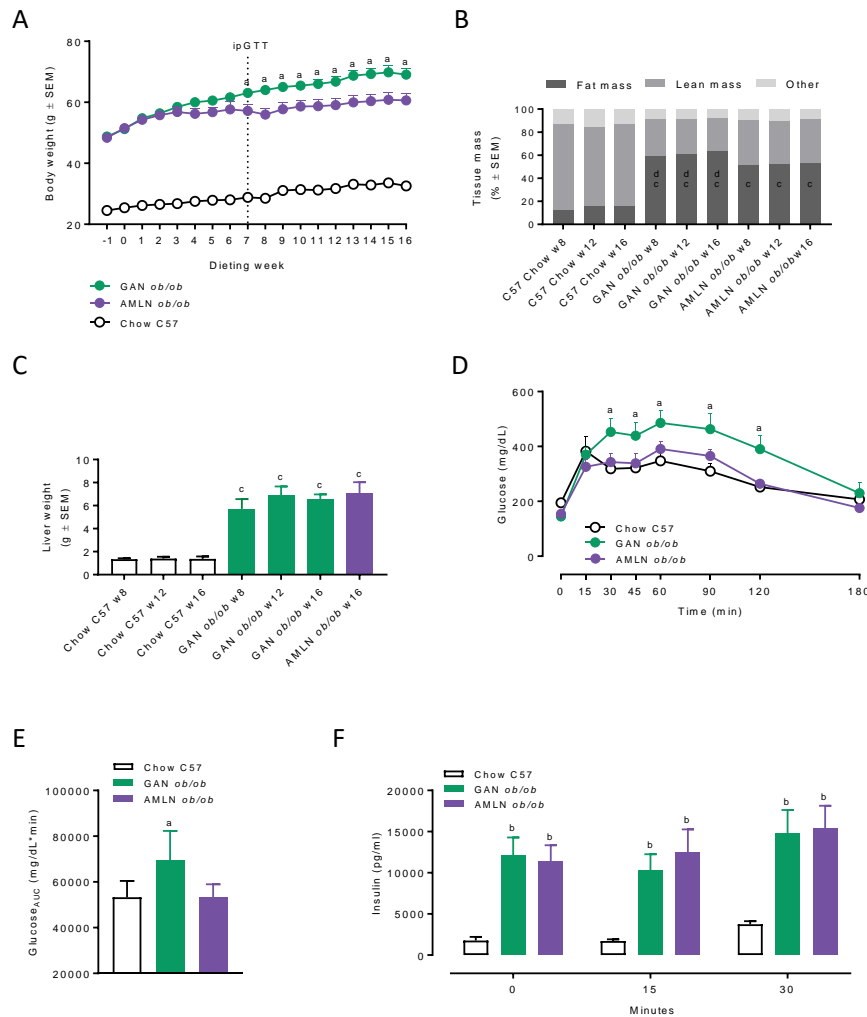


Figure 1 Metabolic parameters in *ob/ob* mice fed amylin liver non-alcoholic steatohepatitis or Gubra amylin non-alcoholic steatohepatitis diet for 8-16 wk. A: Body weight; B: Body composition; C: Terminal liver weight (week 16); D: An intraperitoneal glucose tolerance test was performed in week 7 of the feeding period, glucose excursion curves; E: Area under the curve glucose (area under the curve, 0-180 min); F: Plasma insulin (0, 15, 30 min). ^a*P* < 0.05, ^b*P* < 0.01, ^c*P* < 0.001 *vs* chow-fed C57BL/6J (Chow C57) controls; ^d*P* < 0.001 *vs* amylin liver non-alcoholic steatohepatitis diet (*n* = 5-6 mice per group). AMLN: Amylin liver non-alcoholic steatohepatitis; GAN: Gubra amylin non-alcoholic steatohepatitis; ipGTT: Intraperitoneal glucose tolerance test.

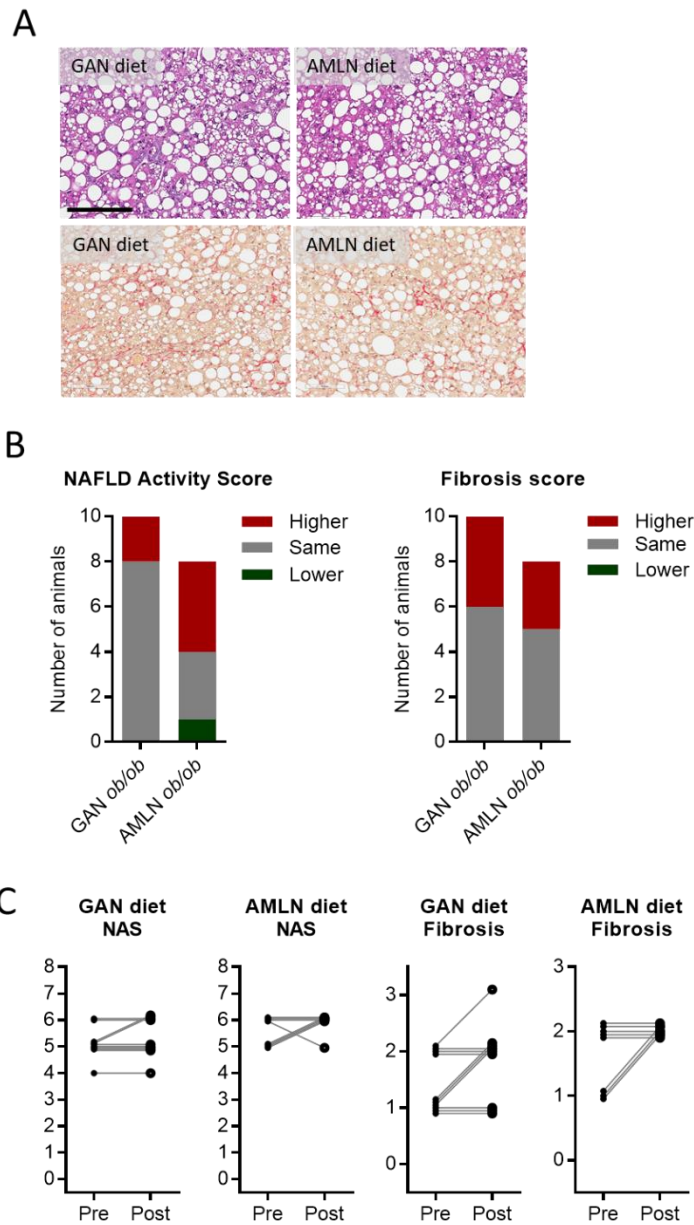


Figure 2 Liver biopsy-confirmed non-alcoholic fatty liver disease activity score and fibrosis scores in *ob/ob* mice fed amylin liver or Gubra amylin non-alcoholic steatohepatitis diet for 16 wk. A: Representative images of terminal liver morphology (upper panel: hematoxylin-eosin staining, lower panel: Picro-Sirius red staining, 20× magnification, scale bar 100 μ m); B: Number of animals with higher, same or lower post-biopsy histopathology score compared to corresponding pre-biopsy score ($n = 8-10$ mice per group). Left panel: Non-alcoholic fatty liver disease activity score (NAS); right panel: Fibrosis score; C: Individual pre-biopsy and terminal NAS and fibrosis scores.

AMLN: Amylin liver non-alcoholic steatohepatitis; GAN: Gubra amylin non-alcoholic steatohepatitis; NAFLD: Non-alcoholic fatty liver disease; NAS: Non-alcoholic fatty liver disease activity score.

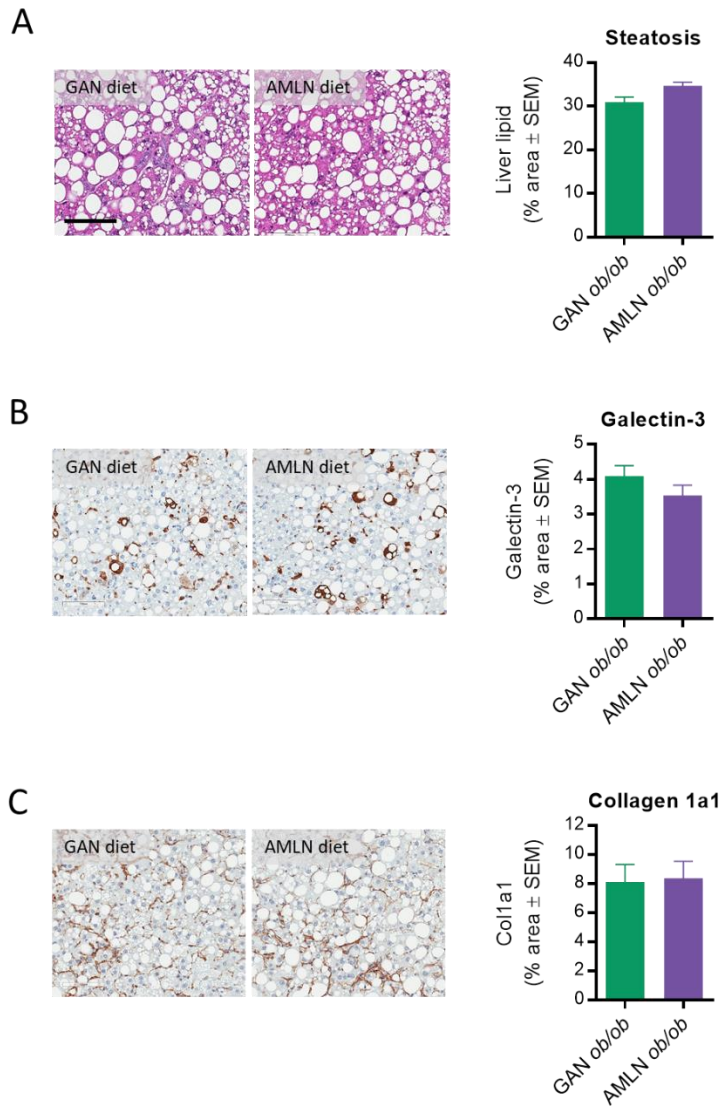


Figure 3 Quantitative histopathological changes in *ob/ob* mice fed amylin liver non-alcoholic steatohepatitis or Gubra amylin non-alcoholic steatohepatitis diet for 16 wk. Fractional (%) area of steatosis (hematoxylin-eosin staining), inflammation [galectin-3 immunostaining and fibrosis (collagen-1a1) immunostaining] determined by imaging-based morphometry ($n = 8-10$ mice per group). A: Steatosis; Galectin-3; C: Collagen-1a1. Scale bar

100 μ m. AMLN: Amylin liver non-alcoholic steatohepatitis; GAN: Gubra amylin non-alcoholic steatohepatitis; Col1a1: Collagen-1a1.

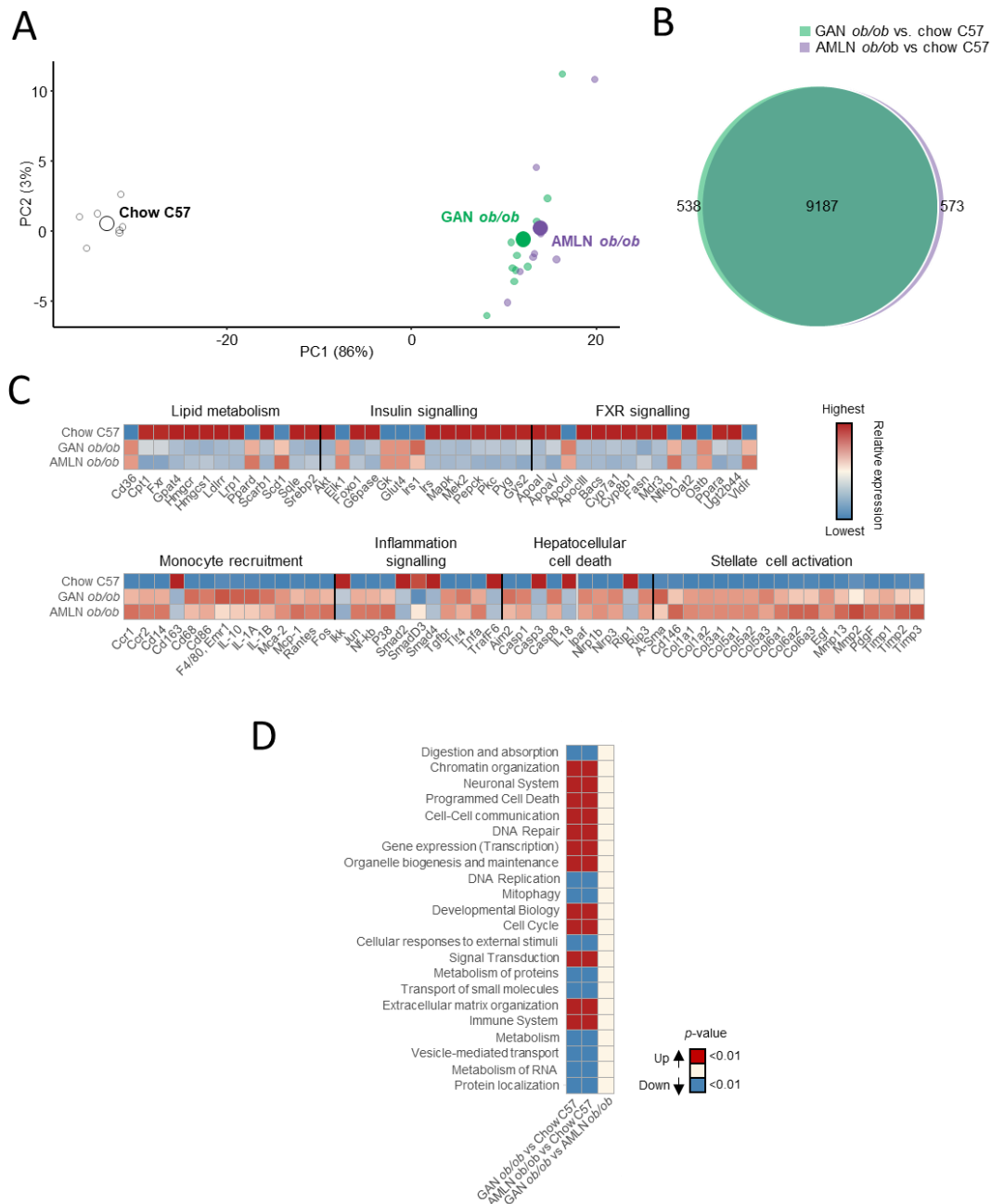


Figure 4 Liver transcriptome changes in *ob/ob* mice fed amylin liver non-alcoholic steatohepatitis or Gubra amylin non-alcoholic steatohepatitis diet for 16 wk. Overview of hepatic gene expression profiles in *ob/ob* mice fed amylin liver non-alcoholic steatohepatitis (NASH) (AMLN) or Gubra amylin non-alcoholic steatohepatitis (GAN) diet compared to age-matched chow-fed

ob/ob mice ($n = 8-10$ mice per group). A: Principal component analysis of samples based on top 500 most variable gene expression levels; B: Group-wise comparison of total number of differentially expressed genes (false discovery rate < 0.05) between *ob/ob* mice fed AMLN or GAN diet for 16 wk *vs* chow-fed C57BL/6J (Chow C57) mice; C: Relative gene expression levels (z-scores) of differentially regulated candidate genes associated with NASH and fibrosis. In-house gene panel on candidate genes is indicated in Supplemental Table 1; D: Group-wise comparison of global liver transcriptome changes according to enrichment of individual gene sets in the Reactome pathway database. Regulated pathways are ranked according to level of statistical significance (P value). AMLN: Amylin liver non-alcoholic steatohepatitis; GAN: Gubra amylin non-alcoholic steatohepatitis; NASH: Non-alcoholic steatohepatitis.

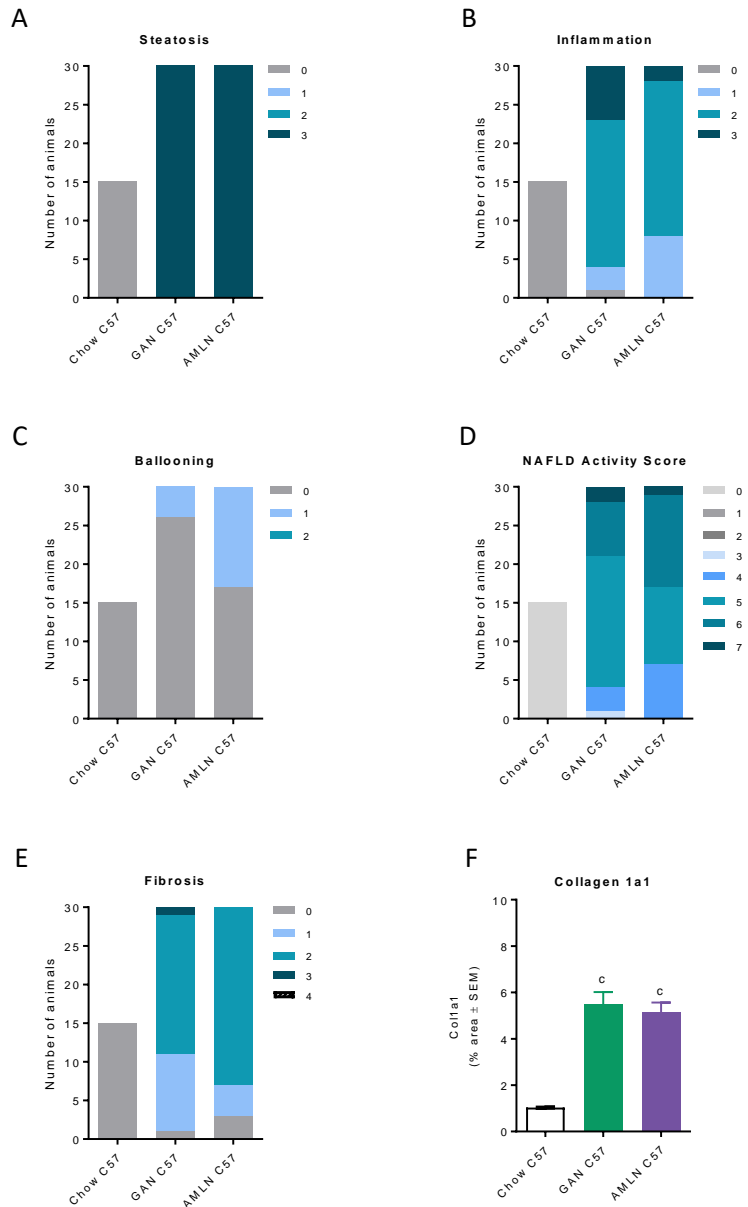


Figure 5 Liver histopathological scores in C57BL/6J mice fed chow, amylin liver non-alcoholic steatohepatitis, or Gubra amylin non-alcoholic steatohepatitis diet for 28 wk. A: Steatosis; B: Lobular inflammation; C: Hepatocyte ballooning; D: Non-alcoholic fatty liver disease activity score; E: Fibrosis; F: Collagen-1a1 fractional area (mean ± SEM). ^c*P* < 0.001 vs chow-fed C57BL/6J (Chow C57) mice.

Table 1 Plasma and liver biomarkers in *ob/ob* mice fed amylin liver non-alcoholic steatohepatitis or Gubra amylin non-alcoholic steatohepatitis diet for 8-16 wk

Group	Weeks on diet	<i>n</i>	ALT (U/L)	AST (U/L)	Plasma (mmol/L)	TG Plasma (mmol/L)	TC	Liver lipid mass (% of liver weight)
Chow C57	8	6	115 ± 60	192 ± 77	1.7 ± 0.2		3.8 ± 0.2	3.5 ± 0.4
	12	6	67 ± 10	93 ± 16	1.7 ± 0.1		3.5 ± 0.1	4.9 ± 0.7
	16	6	61 ± 18	82 ± 18	2.2 ± 0.2		3.8 ± 0.3	3.6 ± 0.4
GAN <i>ob/ob</i>	8	4	913 ± 113 ^a	663 ± 37 ^a	1.2 ± 0.2		11.8 ± 0.9 ^a	31.6 ± 1.3 ^a
	12	5	959 ± 93 ^a	660 ± 52 ^a	1.4 ± 0.1		12.4 ± 1.3 ^a	33.3 ± 0.7 ^a
	16	5	868 ± 102 ^a	674 ± 25 ^{a,d}	1.5 ± 0.2 ^a		14.3 ± 0.8 ^{a,d}	28.4 ± 1.4 ^{a,d}
AMLN <i>ob/ob</i>	16	6	654 ± 39 ^a	399 ± 23 ^a	1.0 ± 0.1 ^a		11.0 ± 0.4 ^a	35.4 ± 0.8 ^{a,d}

^a*P* < 0.05 *vs* chow-fed C57BL/6J (Chow C57) mice. ^d*P* < 0.05 *vs* amylin liver non-alcoholic steatohepatitis *ob/ob* mice.

TC: Total cholesterol; ALT: Alanine aminotransferase; AST: Aspartate aminotransferase; TG: Total triglycerides.